

Dual-Isometric Projected Entangled Pair States

Xie-Hang Yu¹, J. Ignacio Cirac¹, Pavel Kos^{1,*}, and Georgios Styliaris^{1*}

*Max-Planck-Institut für Quantenoptik, Hans-Kopfermann-Str. 1, 85748 Garching, Germany
and Munich Center for Quantum Science and Technology (MCQST), Schellingstr. 4, 80799 München, Germany*



(Received 15 May 2024; accepted 11 September 2024; published 5 November 2024)

Efficient characterization of higher dimensional many-body physical states presents significant challenges. In this Letter, we propose a new class of projected entangled pair states (PEPS) that incorporates two isometric conditions. This new class facilitates the efficient calculation of general local observables and certain two-point correlation functions, which have been previously shown to be intractable for general PEPS, or PEPS with only a single isometric constraint. Despite incorporating two isometric conditions, our class preserves the rich physical structure while enhancing the analytical capabilities. It features a large set of tunable parameters, with only a subleading correction compared to that of general PEPS. Furthermore, we analytically demonstrate that this class can encode universal quantum computation and can represent a transition from topological to trivial order.

DOI: [10.1103/PhysRevLett.133.190401](https://doi.org/10.1103/PhysRevLett.133.190401)

Introduction—Efficiently representing strongly correlated many-body quantum states and extracting their relevant physical properties remain a pivotal challenge in dimensions higher than one. Tensor network methods offer an approach to address this problem. Following the successful application of 1D matrix product states (MPS) [1–3], Ref. [4] introduced their higher-dimensional generalization, projected entangled pair states (PEPS). These states satisfy an entanglement area law [5] and are considered a robust ansatz for representing ground states of gapped local Hamiltonians [6–14]. PEPS also play an important role in quantum dynamics [15–17], statistical mechanics [18–21], the classification of phases [22–25], and quantum machine learning [26–28].

Despite their advantages, finite PEPS still suffer from the rapid growth of the computational resources required for the calculation of physical quantities, such as expectation values of local observables. In practice, even approximate algorithms on finite PEPS are costly and the errors are often hard to control [29–31]. This limitation also holds for translationally invariant systems [32]. It has been shown that the exact contraction of a general PEPS is #P-hard [33], even for typical instances [34], which serves as a fundamental limitation.

One way to address this challenge is to consider some subclass of PEPS. One such class is the isometric PEPS

(iso-PEPS) [35,36], which extends the canonical form of 1D MPS to higher dimensions. Their isometric nature allows for the preparation of all iso-PEPS through sequential unitary circuits [37]. This sequential generation defines a time axis in the iso-PEPS and thus facilitates the backward contraction along this time direction [36]. Despite being typically short-range correlated [38], the iso-PEPS family can capture states with complex correlations, such as topological models and the associated phase transitions [39,40].

However, the computation of the local observables for iso-PEPS is not always efficient. Indeed, this task in two dimensions is shown to be BQP-complete [41], which, subject to standard complexity theory assumptions, indicates that it is hard to simulate classically. Although in principle, some classical algorithms, like the Moses move [36,42], can be used to approximate the result, the errors may remain uncontrolled [43]. This restricts the practical utility of iso-PEPS and motivates the search for new classes of contractible PEPS.

In this Letter, we introduce dual-isometric PEPS (DI-PEPS), a new subclass of iso-PEPS that enhances the computational tractability of tensor networks in higher dimensions, especially for computing local observables and certain two-point correlation functions. The class is defined by imposing an additional isometric condition onto iso-PEPS, which reduces the calculation of the above quantities in the 2D tensor network to a 1D tensor network. The latter is manageable and can be efficiently computed. More broadly, the dual-isometric condition is analogous to dual-unitary gates [44], a class of exactly solvable quantum circuits, and can be seen as a natural extension of these ideas to PEPS. Furthermore, our Letter reveals that the DI-PEPS preserve the rich physical structure of iso-PEPS

*These authors contributed equally to this work.

Published by the American Physical Society under the terms of the Creative Commons Attribution 4.0 International license. Further distribution of this work must maintain attribution to the author(s) and the published article's title, journal citation, and DOI. Open access publication funded by the Max Planck Society.

despite the additional constraint. For this, we show that DI-PEPS can encode universal quantum computations after postselection. As a result, their output probability cannot be efficiently sampled on a classical computer. Additionally, by counting the number of free parameters of DI-PEPS, we show that this number is only reduced at subleading order as compared to conventional PEPS. Lastly, we develop a class of DI-PEPS which exhibits topological order and has a non-trivial transition to decoupled 1D chains. These findings underscore the DI-PEPS as a potent framework for investigating quantum many-body physics, offering new avenues for understanding and manipulating complex quantum systems.

PEPS and the folded picture—We consider PEPS specified by a rank-5 tensor $T_{\text{lb}rt}^p$ for each vertex (x, y) of a 2D square lattice. The index p represents the physical degree of freedom with dimension d , and l, b, r, t (left, bottom, right, top) label the virtual degrees of freedom, each χ dimensional [Fig. 1(a)]. Here $x \in \{1, \dots, N\}$ and $y \in \{1, \dots, M\}$. The wave function is obtained by locally contracting all the virtual degrees of freedom [Fig. 1(b)]. At the boundary, the virtual space is isometrically mapped to the physical space; we explain this choice later. Thus, there are in total $(N + 2) \times (M + 2) - 4$ physical sites.

Our setting and results become more transparent via vectorizing; in graphical notation, this corresponds to “folding” [Fig. 1(c)]. Given a fixed computational basis, an observable is vectorized to $\langle O |$ via $\sum_{ij} O_{ij} |i\rangle\langle j| \mapsto \sum_{ij} O_{ij} \langle i | \langle j |$. States are similarly mapped to a bipartite vector such that

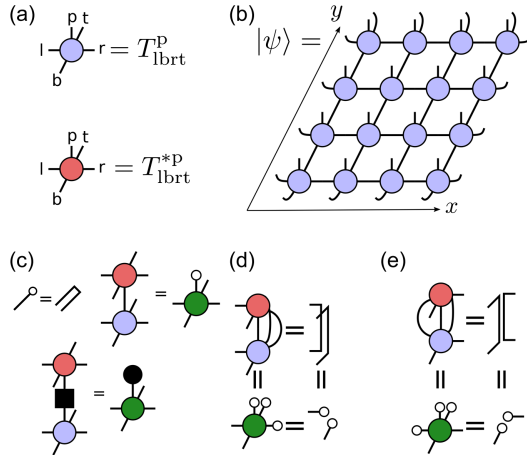
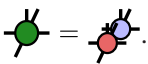


FIG. 1. (a) Rank-5 tensor T of a PEPS. The complex conjugate of T is denoted by T^* . (b) The physical state from the contracted local PEPS tensors, with the virtual space mapped to the physical one on the boundary. (c) The local contraction of bra and ket PEPS states, with its folded notation shown on the right. The bottom panel shows the local expectation value of an observable (black square). The black dot on the right-hand side represents its vectorized form. (d) Isometric condition in the unfolded and folded picture. (e) Dual isometric condition.

$$\langle \psi | \hat{O} | \psi \rangle = \langle O | (| \psi^* \rangle \otimes | \psi \rangle). \quad (1)$$

Graphically, T^* is folded in front of T , thereby forming $T^* \otimes T =$ .

Iso-PEPS—Here we briefly review iso-PEPS [36], which is a subclass of PEPS satisfying the isometric condition

$$\sum_{r,t,p} T_{l_1 b_1 r t}^p T_{l_2 b_2 r t}^{*p} = \delta_{l_1, l_2} \delta_{b_1, b_2}, \quad (2)$$

shown also graphically in Fig. 1(d). This class can be understood as the 2D analog of the canonical form in MPS. Equation (2) directly implies that iso-PEPS can be contracted starting from the top-right direction until an observable is met [36].

Physically, every iso-PEPS tensor can be sequentially generated in depth $\mathcal{O}(N + M)$ via a unitary gate [37]

$$U_{\text{lb}|0}^{\text{prt}} = T_{\text{lb}rt}^p \quad (3)$$

with one of its inputs initialized to $|0\rangle$. Calculating expectation values of local observables in iso-PEPS is as hard as quantum computation since an expectation value of a bulk operator may correspond to a late-time expectation value in the associated sequential circuit; indeed, this task was recently shown to be BQP-complete [41]. Note that the isometric property implies that only a local observable near the bottom or left boundary of the PEPS can be efficiently calculated [36]. In the sequential quantum circuit picture, this only involves a contribution from the gates on the light cone [37].

Dual-isometric PEPS—In this Letter, we introduce a new subclass of iso-PEPS called dual-isometric PEPS (DI-PEPS). This is done by requiring another (dual) isometric condition

$$\sum_{l,t,p} T_{\text{lb}_1 r_1 t}^p T_{\text{lb}_2 r_2 t}^{*p} = \delta_{r_1, r_2} \delta_{b_1, b_2}, \quad (4)$$

as shown in Fig. 1(e). This is in analogy to dual-unitary circuits, where each gate can be interpreted as a valid evolution along a second “time” direction. DI-PEPS thus admit an additional sequential preparation direction. Although we primarily focus on this class, the dual condition of Eq. (4) can be generalized to

$$\sum_{l_1, l_2, t, p} T_{l_1 b_1 r_1 t}^p S_{l_1, l_2} T_{l_2 b_2 r_2 t}^{*p} = S_{r_1, r_2} \delta_{b_1, b_2}, \quad (5)$$

where S is a positive semidefinite matrix (see Ref. [45]). We refer to this enlarged class as *generalized DI-PEPS*.

The key point is that the dual condition, together with Eq. (2), allows an efficient calculation of expectation values of local observables. This becomes transparent in the folded picture, where the expectation value is expressed as

$$\langle \psi | O | \psi \rangle = \text{Diagram (6)} \quad (6)$$

Starting from the top-left corner, we can use Eq. (4)

[Fig. 1(e)] to simplify the configuration as .

This procedure can be iterated, as now the same equation can be used in the next row and column. Following this simplification procedure, one finds that all the tensors on the left and right sides of the observable simplify by Eqs. (4) and (2), respectively, resulting in

$$\langle \psi | O | \psi \rangle = \text{Diagram (7)} \quad (7)$$

This is just a 1D tensor network, which can be efficiently contracted in $\mathcal{O}(M)$. This result also holds for local operators with support larger than 1. In that case, Eq. (7) includes more than one column but with constant (i.e., system-size independent) width.

Our next point of interest is two-point correlation functions, which play a key role in characterizing many-body properties. They can be graphically expressed as

$$\langle \psi | O_1 O_2 | \psi \rangle = \text{Diagram (8)} \quad (8)$$

With the isometric and dual-isometric conditions, one can simplify the diagram from the top-left and top-right corners similarly as before. The final result is

$$\langle \psi | O_1 O_2 | \psi \rangle = \text{Diagram (9)} \quad (9)$$

Here we assume that the two operators are located at (x_1, y_1) and (x_2, y_2) , respectively. The reduced 2D part of the tensor network is of size $t_1 \times t_2$, with $t_1 = |x_2 - x_1|$ and $t_2 = \min\{y_1, y_2\}$. If either t_1 or t_2 is constant, the correlator still reduces to an efficiently contractible 1D tensor network with a possibly increased, but constant, bond dimension. Similar as above, the generalized DI-PEPS (5) preserve the solvability of 1- and 2-point correlations, see Ref. [45].

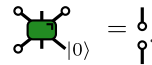
Not only in our case but also in general, the calculation of local or multipoint expectation values in 2D PEPS can be interpreted as a circuit of 1 + 1D completely positive maps acting over the virtual space; in general, however, these are not trace-preserving. This is established by interpreting tensor-network diagrams, such as the one in Eq. (8), along a 45° counterclockwise rotated direction, and defining Kraus operators (indexed by p) as $E_{\text{tr,lb}}^p = T_{\text{lbrt}}^p$. Pictorially, this can be expressed as

$$\text{Diagram (10)} = \text{Diagram (10)}, \quad (10)$$

where the right side depicts the completely positive map in the folded picture. For the case of iso-PEPS, this map is in addition trace-preserving, i.e., it corresponds to a physical evolution. From this point of view, the solvability of DI-PEPS can be connected with the simplifying properties of two-unital space channels from Ref. [54].

The boundary condition of Fig. 1(b) also obtains a physical interpretation at this stage. Viewing the PEPS as a quantum circuit, the boundary conditions correspond to initially preparing $N + M$ EPR-pairs, and inputting half of each pair to the circuit.

Examples of DI-PEPS—First, a known special subfamily of DI-PEPS is perfect tensors [55–57], and their generalizations [58], originally developed in the context of the AdS/CFT correspondence. However, this subfamily requires an isometric condition under any bipartition, which is a much stronger constraint than that of generic DI-PEPS. Second, sequentially generated states (SGS) [59] are also a subfamily of generalized DI-PEPS from Eq. (5) (see Ref. [45]).

As mentioned in Eq. (3), DI-PEPS can be prepared with a sequential quantum circuit with the additional condition $\sum_{\text{ptl}} U_{\text{lb}_1(0)}^{\text{pr}_1\text{t}} (U_{\text{lb}_2(0)}^{\text{pr}_2\text{t}})^* = \delta_{\text{b}_1, \text{b}_2} \delta_{\text{r}_1, \text{r}_2}$, pictorially expressed as . Some classes of unitary gates satisfying the above are:

Permutation-phase gates: $U = P_{231} D$ composed with arbitrary single site gates, where P_{231} is the shift-permutation $P_{231} = \text{Diagram}$ and D is an arbitrary diagonal gate in the computational basis. This family generalizes dual-unitary gates, for which P_{21} is just the SWAP [44], to a tripartite setting.

3-qubit gates ($d = \chi = 2$): We take a nonexhaustive ansatz $U = \prod_{\alpha} \exp(iQ_{\alpha} \sigma_2^{\alpha} \sigma_3^{\alpha}) \prod_{\beta} \exp(iJ_{\beta} \sigma_1^{\beta} \sigma_2^{\beta})$, where α, β run

over 1,2,3 and σ_m^α is the α Pauli matrix acting on the m th qubit. We find that $Q_1 = 0, Q_2 = \pi/4, J_3 = \pi/4$ or $Q_2 = \pi/4, \cos 2J_1 \cos 2Q_3 = \cos 2J_2 \cos 2Q_3 = 0$ satisfies the condition. Additional arbitrary single site unitaries on all five legs but the ancillary one associated with $|0\rangle$ are allowed.

Controlled-dual unitaries: $U_{\text{lba}}^{\text{prt}} = (1/\sqrt{d}) \sum_i |i\rangle_p \langle i|_a V_{\text{tr,lb}}^i$, composed with arbitrary single site gates, where V^i is a dual-unitary gate [44], i.e., it is unitary and also satisfies $\sum_{\text{tl}} V_{\text{tr}_1, \text{lb}_1}^i V_{\text{tr}_2, \text{lb}_2}^{*i} = \delta_{r_1, r_2} \delta_{b_1, b_2}$. More generally, any triunitary quantum gate [60] and multidirectional unitary gate (after grouping some indices) [61] is an example generating DI-PEPS.

Next, we discuss another interesting example, which is not constructed from unitary gates, but from the “plumbing tensor” [40] which is a special PEPS with $D = \chi^4$. The local tensor $T_{\text{lbrt}}^{\text{p}}$ is determined by another rank-4 tensor W as

$$T_{\text{lbrt}}^{\text{p}} = T_{\text{lbrt}}^{\text{p}_1 \text{p}_2 \text{p}_3 \text{p}_4} = \delta_{l, \text{p}_1} \delta_{b, \text{p}_2} \delta_{r, \text{p}_3} \delta_{t, \text{p}_4} W_{\text{lbrt}}, \quad (11)$$

where $\text{p}_i = 1, \dots, \chi$. Graphically,  with  denoting the delta tensor which is nonvanishing only if all three legs take the same value. The elements of the W matrix are restricted by Eqs. (2) and (4) (see Ref. [45] for its specific form). Now, if we place the W tensor at the vertices of a square lattice, the physical degrees of freedom lay on the edges [62]. Notably, the simplest case $\chi = 2$ includes the toric code tensor [40,63] as an example of DI-PEPS. We will return to the topological properties of this class later.

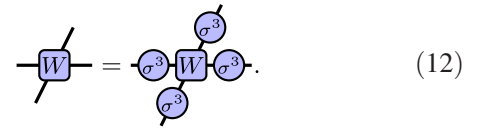
Parameter counting and computational complexity— Here we argue about the richness of DI-PEPS, despite them having analytically accessible correlation functions. As with every PEPS, the representation of the state in terms of tensors is nonunique. We take into account this so-called gauge freedom by introducing a corresponding canonical form for the family of generalized DI-PEPS [see Eq. (5) and [45]]. The resulting number of free real parameters of a normal [64] generalized DI-PEPS (formed by repeating the same tensor) is $2(d-1)\chi^4$. Compared to the number of free real parameters $2d\chi^4 - 4\chi^2 + 2$ of a normal PEPS [45], we see that DI-PEPS cover a large subclass of normal PEPS.

Parameter counting and computational complexity— Here we argue about the richness of DI-PEPS, despite them having analytically accessible correlation functions. As with every PEPS, the representation of the state in terms of tensors is nonunique. We take into account this so-called gauge freedom by introducing a corresponding canonical form for the family of generalized DI-PEPS [see Eq. (5) and [45]]. The resulting number of free real parameters of a normal [64] generalized DI-PEPS (formed by repeating the same tensor) is $2(d-1)\chi^4$. Compared to the number of free real parameters $2d\chi^4 - 4\chi^2 + 2$ of a normal PEPS [45], we see that DI-PEPS cover a large subclass of normal PEPS.

We further consider the computational complexity of DI-PEPS. Although one- and two-point correlators can be efficiently computed, we demonstrate that sampling of a DI-PEPS cannot be efficiently simulated in a classical computer. Following Ref. [41], we show that the DI-PEPS can encode universal quantum computations with postselection. Thus, according to Ref. [65], the output probability distribution cannot be sampled to a multiplicative precision by a classical computer efficiently, unless the polynomial hierarchy collapses to its third level, i.e., $\text{postBQP} = \text{postBPP}$. While the proof and further discussion are available in [45], here we sketch the main points. Based on the previous discussion, we can interpret

the PEPS as a 1 + 1D quantum circuit in the virtual (bond) space, while at the last layer the boundary bond outputs the computation result to physical space. We choose the DI-PEPS constructed from the controlled-dual-unitary gates (example above), thus we encode a dual-unitary circuit into the DI-PEPS. The result follows since the dual-unitary circuits are universal with postselection [66]. This computational complexity also persists for DI-PEPS with further symmetry constraints, such as global $U(1)$ symmetry [45]. This is achieved by encoding the above construction into a single block of the symmetric DI-PEPS.

DI-PEPS, topological states, and locality— In this section, we consider in detail a $\chi = 2$ subfamily of the DI-PEPS constructed from the plumbing tensor of Eq. (11), with a special focus on its topological properties. To this end, we impose a \mathbb{Z}_2 symmetry on the W tensor

$$\text{Diagram of } W \text{ tensor with } \sigma^3 \text{ symmetry} = \text{Diagram of } W \text{ tensor with } \sigma^3 \text{ symmetry.} \quad (12)$$


This symmetry restricts its form to

$$W_{\text{lbrt}} = \begin{pmatrix} \sqrt{\alpha} & & & \sqrt{1-\alpha} \\ & \sqrt{\beta} & \sqrt{1-\beta} & \\ & \sqrt{1-\alpha} & \sqrt{\alpha} & \\ \sqrt{1-\beta} & & & \sqrt{\beta} \end{pmatrix}, \quad (13)$$

with $\alpha, \beta \in [0, 1]$, where we omit the complex phases of each element since they are irrelevant to the topological degeneracy.

Our aim is to probe the topological order of the above subfamily. Each PEPS corresponds to a ground state of a local parent Hamiltonian [2]. A PEPS is said to be topologically ordered if the parent Hamiltonian has topological degeneracy in its ground state subspace, which can be characterized by the transfer operator \mathbb{T} [24,67]. Parallel to Ref. [24], here we put the PEPS on a cylinder. We cut out one loop around the cylinder and contract it with its complex conjugate over the physical degrees to form the transfer operator in the doubled virtual space,

$$\mathbb{T} = \text{Diagram of transfer operator } \mathbb{T} \text{ on a cylinder.} \quad (14)$$


According to the \mathbb{Z}_2 symmetry, the transfer operator can be block diagonalized into $\mathbb{T}_{p, \phi}^{p', \phi'}$, where p, p' denote the parity of the ket and bra state, respectively; $\phi, \phi' = 0, \pi$ denote whether a flux is threading the cylinder, i.e., if an additional σ^3 is present in the ket and (or) bra virtual space. Because of

the delta tensor in Eq. (11), we immediately see that $p = p'$ and the transformation $\phi(\phi') \rightarrow \phi(\phi') + \pi$ does not change the transfer operator. Thus, we only need to distinguish four transfer operators $\mathbb{T}_{e\phi}^{e\phi}, \mathbb{T}_{o\phi}^{o\phi}, \mathbb{T}_{e\phi}^{e\phi+\pi}, \mathbb{T}_{o\phi}^{o\phi+\pi}$.

The key point is that the leading eigenvalues $\lambda_{p\phi}^{p\phi}$ and the corresponding degeneracy in each block determine the topological properties of the tensor. This is since they encode, in the thermodynamic limit, the inner product of the states corresponding to different choices of p, ϕ , which indicates anyon condensation and confinement [68].

If $\alpha = \beta = \frac{1}{2}$, the resulting state is the toric code [40,63] with nontrivial topological order. At this point, $|\lambda_{e\phi}^{e\phi}| = |\lambda_{o\phi}^{o\phi}| = 1, |\lambda_{e\phi}^{e\phi+\pi}| = |\lambda_{o\phi}^{o\phi+\pi}| = 0$ and the blocks with the largest eigenvalues, $\mathbb{T}_{e\phi}^{e\phi}, \mathbb{T}_{o\phi}^{o\phi}$ are nondegenerate. The lines $\alpha = 1$ or $\beta = 1$, and the point $\alpha = \beta = 0$ are in the trivial phase, since they correspond to decoupled 1D chains, each in a GHZ state. Those points have exponentially many degeneracies in the leading eigenvalues of the transfer operators $\mathbb{T}_{e\phi}^{e\phi}, \mathbb{T}_{o\phi}^{o\phi}$ with respect to the vertical length M and we refer to them as the GHZ points. In the Supplemental Material [45], we moreover analytically show that except for the GHZ points mentioned above, it always holds that $|\lambda_{e\phi}^{e\phi}| = |\lambda_{o\phi}^{o\phi}| > |\lambda_{e\phi}^{e\phi+\pi}| = |\lambda_{o\phi}^{o\phi+\pi}|$ and the blocks with the largest eigenvalues, $\mathbb{T}_{e\phi}^{e\phi}, \mathbb{T}_{o\phi}^{o\phi}$ are nondegenerate. We achieve that by mapping it to a frustration-free Hamiltonian. We also calculate the full spectrum of the transfer operators along the line $\alpha = \beta$ or $\alpha = 1 - \beta$ in [45]. Thus we can conclude that the DI-PEPS of Eq. (13) exhibit the same topological phase as the toric code, except from the GHZ points. At those points we have a crossing from a topological phase with degeneracy 4 to a decoupled phase with exponentially many degeneracies. This explicitly demonstrates that DI-PEPS contain topological phases.

Another interesting question is the locality of parent Hamiltonians for a given family of PEPS. Note that even states with long-range topological order [63,69,70] admit local parent Hamiltonians. In principle, the parent Hamiltonian can be obtained by blocking [2], which, however, may lead to terms with larger supports. For example, if $d = \chi = 2$, generally it is sufficient to block 4×5 tensors and the resulting parent Hamiltonian is locally supported on these 20 sites, which can be slightly decreased by a costly numerical procedure [71]. Our examples from Eq. (13) with nonvanishing α, β admit an analytical form of the parent Hamiltonians which are at most 8-local. In particular, if $\alpha = 1 - \beta$, this can be improved to a 4-local Hamiltonian. We illustrate the latter here while the general case follows a similar argument [45]. The state with $\alpha = 1 - \beta$ can be obtained by acting with a single-body operator $\mathcal{U}_v = e^{s\sigma^3}$ on each vertical edge of the toric code, with $s = \frac{1}{4} \ln[\alpha/(1-\alpha)]$. Thus, the parent Hamiltonian of our state can be related to the toric code one via the transformation $h = \prod_v \mathcal{U}_v^{-1\dagger} h_{\text{TC}} \mathcal{U}_v^{-1}$. Here h

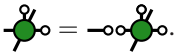
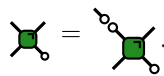
and h_{TC} are local terms of the parent Hamiltonians of our state and the toric code, respectively, and v belongs to the vertical edges which overlap with h_{TC} . The above transformation does not change the locality of h which remains 4 as for h_{TC} [63].

Discussion and outlook—In this Letter, we proposed a new class of PEPS called DI-PEPS, with two isometric conditions. These PEPS allow for efficient computations of local and certain two-point correlation functions. Furthermore, we have shown that this class exhibits interesting physical properties. It has a large number of free parameters, encodes universal quantum computation after postselection and can represent interesting transitions from topological to trivial order.

It remains an important open question how well the DI-PEPS perform as an ansatz for variational methods, both for ground states and the dynamics. On one hand, the restriction from PEPS to DI-PEPS decreases expressivity. On the other hand the efficient way to obtain reduced density matrices allows for bigger bond dimensions.

Let us now discuss possible generalizations. We imposed isometric conditions from top-right and top-left. Actually, one can rotate the tensor and consider the isometric conditions from any two adjacent corners, e.g., top-right and bottom-right. As with iso-PEPS [36], different choices can be made in different parts of the state. However, if one considers the isometric conditions from two diagonal corners (e.g., top-right and bottom-left), the expectation values of local observables are simplified to a contraction of a single tensor. Thus, we expect this class to be less expressive.

Moreover, we can impose additional isometric conditions, from bottom-left and (or) bottom-right. In this case, higher-point correlation functions are also tractable. One can figure out that for a PEPS with n -isometric conditions, all the $(n-1)$ -point correlation functions are solvable. Although in our Letter we focus on the 2D square lattice, the generalization to higher dimensions or different lattices is also interesting. We may consider the 3D simple cubic lattice, or the triangle lattice where one can define up to six isometric conditions.

Lastly, the equivalence between PEPS and 1 + 1D quantum completely positive maps may guide us to construct new classes of solvable local quantum evolutions for any solvable PEPS. As an example, we look at sequentially generated states (SGS) [59], which satisfy . We can use our proposed duality to define a new kind of solvable quantum maps with the property . This class allows the efficient calculation of local and two-point expectation values (see also [72]). Importantly, this class is solvable even for nontrace preserving dynamics, for example, including measurements.

Acknowledgments—The authors thank Giacomo Giudice, Yu-Jie Liu, Daniel Malz, Frank Pollmann,

Balázs Pozsgay, and Rahul Trivedi for fruitful discussions. The research is part of the Munich Quantum Valley, which is supported by the Bavarian state government with funds from the Hightech Agenda Bayern Plus. The authors acknowledge funding from the projects FermiQP of the Bildungsministerium für Bildung und Forschung (BMBF). P. K. acknowledges financial support from the Alexander von Humboldt Foundation.

-
- [1] M. Fannes, B. Nachtergaele, and R. F. Werner, Finitely correlated states on quantum spin chains, *Commun. Math. Phys.* **144**, 443 (1992).
- [2] J. I. Cirac, D. Pérez-García, N. Schuch, and F. Verstraete, Matrix product states and projected entangled pair states: Concepts, symmetries, theorems, *Rev. Mod. Phys.* **93**, 045003 (2021).
- [3] J. Haegeman and F. Verstraete, Diagonalizing transfer matrices and matrix product operators: A medley of exact and computational methods, *Annu. Rev. Condens. Matter Phys.* **8**, 355 (2017).
- [4] F. Verstraete and J. I. Cirac, Renormalization algorithms for quantum-many body systems in two and higher dimensions, [arXiv:cond-mat/0407066](https://arxiv.org/abs/cond-mat/0407066).
- [5] J. Eisert, M. Cramer, and M. B. Plenio, Colloquium: Area laws for the entanglement entropy, *Rev. Mod. Phys.* **82**, 277 (2010).
- [6] H. Niggemann, A. Klümper, and J. Zittartz, Quantum phase transition in spin-3/2 systems on the hexagonal lattice—optimum ground state approach, *Z. Phys. B Condens. Matter* **104**, 103 (1997).
- [7] F. Verstraete and J. I. Cirac, Matrix product states represent ground states faithfully, *Phys. Rev. B* **73**, 094423 (2006).
- [8] F. Verstraete, M. M. Wolf, D. Perez-Garcia, and J. I. Cirac, Criticality, the area law, and the computational power of projected entangled pair states, *Phys. Rev. Lett.* **96**, 220601 (2006).
- [9] M. B. Hastings, An area law for one-dimensional quantum systems, *J. Stat. Mech.* (2007) P08024.
- [10] F. G. Brandao and M. Horodecki, Exponential decay of correlations implies area law, *Commun. Math. Phys.* **333**, 761 (2015).
- [11] A. Molnar, N. Schuch, F. Verstraete, and J. I. Cirac, Approximating Gibbs states of local Hamiltonians efficiently with projected entangled pair states, *Phys. Rev. B* **91**, 045138 (2015).
- [12] A. Anshu, A. W. Harrow, and M. Soleimanifar, Entanglement spread area law in gapped ground states, *Nat. Phys.* **18**, 1362 (2022).
- [13] A. Anshu, I. Arad, and D. Gosset, An area law for 2d frustration-free spin systems, in *Proceedings of the 54th Annual ACM SIGACT Symposium on Theory of Computing* (Association for Computing Machinery, New York, 2022), pp. 12–18.
- [14] M. J. O’Rourke and G. K.-L. Chan, Entanglement in the quantum phases of an unfrustrated Rydberg atom array, *Nat. Commun.* **14**, 5397 (2023).
- [15] I. Pižorn, L. Wang, and F. Verstraete, Time evolution of projected entangled pair states in the single-layer picture, *Phys. Rev. A* **83**, 052321 (2011).
- [16] R. T. Ponnaganti, M. Mambrini, and D. Poilblanc, Real-time dynamics of a critical resonating valence bond spin liquid, *Phys. Rev. B* **106**, 195132 (2022).
- [17] R. T. Ponnaganti, M. Mambrini, and D. Poilblanc, Tensor network variational optimizations for real-time dynamics: Application to the time-evolution of spin liquids, *SciPost Phys.* **15**, 158 (2023).
- [18] M. Levin and C. P. Nave, Tensor renormalization group approach to two-dimensional classical lattice models, *Phys. Rev. Lett.* **99**, 120601 (2007).
- [19] Z. Y. Xie, H. C. Jiang, Q. N. Chen, Z. Y. Weng, and T. Xiang, Second renormalization of tensor-network states, *Phys. Rev. Lett.* **103**, 160601 (2009).
- [20] H. H. Zhao, Z. Y. Xie, Q. N. Chen, Z. C. Wei, J. W. Cai, and T. Xiang, Renormalization of tensor-network states, *Phys. Rev. B* **81**, 174411 (2010).
- [21] H.-H. Zhao, Z.-Y. Xie, T. Xiang, and M. Imada, Tensor network algorithm by coarse-graining tensor renormalization on finite periodic lattices, *Phys. Rev. B* **93**, 125115 (2016).
- [22] X. Chen, Z.-C. Gu, and X.-G. Wen, Classification of gapped symmetric phases in one-dimensional spin systems, *Phys. Rev. B* **83**, 035107 (2011).
- [23] N. Schuch, D. Pérez-García, and I. Cirac, Classifying quantum phases using matrix product states and projected entangled pair states, *Phys. Rev. B* **84**, 165139 (2011).
- [24] N. Schuch, D. Poilblanc, J. I. Cirac, and D. Pérez-García, Topological order in the projected entangled-pair states formalism: Transfer operator and boundary Hamiltonians, *Phys. Rev. Lett.* **111**, 090501 (2013).
- [25] P. Corboz, P. Czarnik, G. Kapteijns, and L. Tagliacozzo, Finite correlation length scaling with infinite projected entangled-pair states, *Phys. Rev. X* **8**, 031031 (2018).
- [26] Z. Liu, Q. Ye, L.-W. Yu, L. M. Duan, and D.-L. Deng, Theory on variational high-dimensional tensor networks, [arXiv:2303.17452](https://arxiv.org/abs/2303.17452).
- [27] S. Cheng, L. Wang, and P. Zhang, Supervised learning with projected entangled pair states, *Phys. Rev. B* **103**, 125117 (2021).
- [28] A. Azizi, K. Najafi, M. Mohseni, and C. A. Venice, Learning phase transition in Ising model with tensor-network Born machines, in *34th Conference on Neural Information Processing Systems, First Workshop on Quantum Tensor Networks in Machine Learning* (Neural Information Processing Systems Foundation, Inc. (NeurIPS), 2020).
- [29] M. Lubasch, J. I. Cirac, and M.-C. Bañuls, Algorithms for finite projected entangled pair states, *Phys. Rev. B* **90**, 064425 (2014).
- [30] M. Lubasch, J. I. Cirac, and M.-C. Bañuls, Unifying projected entangled pair state contractions, *New J. Phys.* **16**, 033014 (2014).
- [31] G. Scarpa, A. Molnár, Y. Ge, J. J. García-Ripoll, N. Schuch, D. Pérez-García, and S. Iblisdir, Projected entangled pair states: Fundamental analytical and numerical limitations, *Phys. Rev. Lett.* **125**, 210504 (2020).
- [32] L. Vanderstraeten, J. Haegeman, P. Corboz, and F. Verstraete, Gradient methods for variational optimization of projected entangled-pair states, *Phys. Rev. B* **94**, 155123 (2016).

- [33] N. Schuch, M. M. Wolf, F. Verstraete, and J. I. Cirac, Computational complexity of projected entangled pair states, *Phys. Rev. Lett.* **98**, 140506 (2007).
- [34] J. Haferkamp, D. Hangleiter, J. Eisert, and M. Gluza, Contracting projected entangled pair states is average-case hard, *Phys. Rev. Res.* **2**, 013010 (2020).
- [35] R. Haghshenas, M. J. O'Rourke, and Garnet Kin-Lic Chan, Conversion of projected entangled pair states into a canonical form, *Phys. Rev. B* **100**, 054404 (2019).
- [36] M. P. Zaletel and F. Pollmann, Isometric tensor network states in two dimensions, *Phys. Rev. Lett.* **124**, 037201 (2020).
- [37] Z.-Y. Wei, D. Malz, and J. I. Cirac, Sequential generation of projected entangled-pair states, *Phys. Rev. Lett.* **128**, 010607 (2022).
- [38] D. Haag, F. Baccari, and G. Styliaris, Typical correlation length of sequentially generated tensor network states, *PRX Quantum* **4**, 030330 (2023).
- [39] T. Soejima, K. Siva, N. Bultinck, S. Chatterjee, F. Pollmann, and M. P. Zaletel, Isometric tensor network representation of string-net liquids, *Phys. Rev. B* **101**, 085117 (2020).
- [40] Y.-J. Liu, K. Shtengel, and F. Pollmann, Topological quantum phase transitions in 2d isometric tensor networks, [arXiv:2312.05079](https://arxiv.org/abs/2312.05079).
- [41] D. Malz and R. Trivedi, Computational complexity of isometric tensor network states, [arXiv:2402.07975](https://arxiv.org/abs/2402.07975).
- [42] Y. Wu, S. Anand, S.-H. Lin, F. Pollmann, and M. P. Zaletel, Two-dimensional isometric tensor networks on an infinite strip, *Phys. Rev. B* **107**, 245118 (2023).
- [43] S.-H. Lin, M. P. Zaletel, and F. Pollmann, Efficient simulation of dynamics in two-dimensional quantum spin systems with isometric tensor networks, *Phys. Rev. B* **106**, 245102 (2022).
- [44] B. Bertini, P. Kos, and T. Prosen, Exact correlation functions for dual-unitary lattice models in $1 + 1$ dimensions, *Phys. Rev. Lett.* **123**, 210601 (2019).
- [45] See Supplemental Material at <http://link.aps.org/supplemental/10.1103/PhysRevLett.133.190401> for details, which includes Refs. [46–53].
- [46] L. Piroli, B. Bertini, J. I. Cirac, and T. Prosen, Exact dynamics in dual-unitary quantum circuits, *Phys. Rev. B* **101**, 094304 (2020).
- [47] R. Raussendorf, D. E. Browne, and H. J. Briegel, Measurement-based quantum computation on cluster states, *Phys. Rev. A* **68**, 022312 (2003).
- [48] M. A. Nielsen and I. L. Chuang, *Quantum computation and Quantum Information* (Cambridge University Press, Cambridge, England, 2010).
- [49] A. Molnar, J. Garre-Rubio, D. Pérez-García, N. Schuch, and J. I. Cirac, Normal projected entangled pair states generating the same state, *New J. Phys.* **20**, 113017 (2018).
- [50] D. Pérez-García, M. Sanz, C. Gonzalez-Guillen, M. M. Wolf, and J. I. Cirac, Characterizing symmetries in a projected entangled pair state, *New J. Phys.* **12**, 025010 (2010).
- [51] M. M. Wolf, Quantum channels and operations-guided tour (2012), <https://mediatum.ub.tum.de/doc/1701036/document.pdf>.
- [52] S. Singh, R. N. C. Pfeifer, and G. Vidal, Tensor network states and algorithms in the presence of a global $U(1)$ symmetry, *Phys. Rev. B* **83**, 115125 (2011).
- [53] B. Bauer, P. Corboz, R. Orús, and M. Troyer, Implementing global Abelian symmetries in projected entangled-pair state algorithms, *Phys. Rev. B* **83**, 125106 (2011).
- [54] P. Kos and G. Styliaris, Circuits of space and time quantum channels, *Quantum* **7**, 1020 (2023).
- [55] F. Pastawski, B. Yoshida, D. Harlow, and J. Preskill, Holographic quantum error-correcting codes: Toy models for the bulk/boundary correspondence, *J. High Energy Phys.* **06** (2015) 149.
- [56] G. Evenbly, Hyperinvariant tensor networks and holography, *Phys. Rev. Lett.* **119**, 141602 (2017).
- [57] M. Steinberg and J. Prior, Conformal properties of hyperinvariant tensor networks, *Sci. Rep.* **12**, 532 (2022).
- [58] M. Steinberg, S. Feld, and A. Jahn, Holographic codes from hyperinvariant tensor networks, *Nat. Commun.* **14**, 7314 (2023).
- [59] M. C. Bañuls, D. Pérez-García, M. M. Wolf, F. Verstraete, and J. I. Cirac, Sequentially generated states for the study of two-dimensional systems, *Phys. Rev. A* **77**, 052306 (2008).
- [60] C. Jonay, V. Khemani, and M. Ippoliti, Triunitary quantum circuits, *Phys. Rev. Res.* **3**, 043046 (2021).
- [61] M. Mestyán, B. Pozsgay, and I. M. Wanless, Multi-directional unitarity and maximal entanglement in spatially symmetric quantum states, *SciPost Phys.* **16**, 010 (2024).
- [62] Each edge hosts two spins that can be merged into a single one by $\sum_{i=1}^{\chi} |i\rangle\langle ii|$.
- [63] A. Y. Kitaev, Fault-tolerant quantum computation by anyons, *Ann. Phys. (Amsterdam)* **303**, 2 (2003).
- [64] A PEPS tensor is called normal if it becomes injective after blocking. Generic PEPS are normal [2].
- [65] M. J. Bremner, R. Jozsa, and D. J. Shepherd, Classical simulation of commuting quantum computations implies collapse of the polynomial hierarchy, *Proc. R. Soc. A* **467**, 459 (2011).
- [66] R. Suzuki, K. Mitarai, and K. Fujii, Computational power of one- and two-dimensional dual-unitary quantum circuits, *Quantum* **6**, 631 (2022).
- [67] N. Schuch, I. Cirac, and D. Pérez-García, Peps as ground states: Degeneracy and topology, *Ann. Phys. (Amsterdam)* **325**, 2153 (2010).
- [68] J. Haegeman, V. Zauner, N. Schuch, and F. Verstraete, Shadows of anyons and the entanglement structure of topological phases, *Nat. Commun.* **6**, 8284 (2015).
- [69] M. A. Levin and X.-G. Wen, String-net condensation: A physical mechanism for topological phases, *Phys. Rev. B* **71**, 045110 (2005).
- [70] Z.-C. Gu, M. Levin, B. Swingle, and X.-G. Wen, Tensor-product representations for string-net condensed states, *Phys. Rev. B* **79**, 085118 (2009).
- [71] G. Giudici, J. I. Cirac, and N. Schuch, Locality optimization for parent Hamiltonians of tensor networks, *Phys. Rev. B* **106**, 035109 (2022).
- [72] H.-R. Wang, X.-Y. Yang, and Z. Wang, Exact hidden Markovian dynamics in quantum circuits, *Phys. Rev. Lett.* **133**, 170402 (2024).